CFSRC COLLOQUIUM

Proceedings of the Cold-Formed Steel Research Consortium Colloquium
17-19 October 2022 (cfsrc.org)

Effects of Modeling Decisions on the Lateral Performance of Cold-Formed Steel Framed Walls

Zhidong Zhang[1], Matthew S. Speicher[2], Amanpreet Singh[3], Tara C. Hutchinson[4], Benjamin W. Schafer[5]

Abstract

This study proposes a modeling protocol for the lateral performance of cold-formed steel (CFS) framed wall-lines that contain both steel sheet sheathed shear walls as well as gravity walls and may include the impact of non-structural finish on these wall-lines. For example, a common structural detail that impacts the lateral performance of wall-lines is the presence of a ledger track used to connect the floor system to the wall. Ledger tracks or similar end joists are common in wall-lines in buildings, but almost never present in shear wall experimental testing programs. In addition, a common non-structural detail impacting wall-line lateral performance is the type of finish system (e.g., gypsum board). In conventional CFS lateral design, all non-structural and many structural details are ignored, thus underestimating the strength and potentially the ductility. A numerical study employing OpenSeesPy is validated against a unique set of wall-line tests and then exercised with or without ledger tracks, as well as with or without finishes, herein. The model is also applied to an unsymmetric wall-line to examine the impact of the location of shear walls within a wall-line on the strength and ductility as well as the demands on connecting elements. The modeling results characterize the degree by which both strength and ductility of wall-lines can increase due to the presence of a ledger track and/or finish system. A sensitivity analysis is conducted to explore the effects of various additional wall-line details, including track bending stiffness, bottom track shear anchor spacing, and magnitude of gravity loading. The developed OpenSeesPy model can capture the impact of detailing and reveal the effects of wall-line configurations, thus this modeling framework can be further incorporated into building-level numerical studies.

1. Introduction

Beneficial characteristics of cold-formed steel (CFS) framed building structures including lightweight, low cost, multi-hazard resilience, and sustainability make it a competitive solution among low-rise and mid-rise building construction. CFS framed shear walls with sheathed panels, CFS framed strap-braced walls, and CFS steel special bolted moment frames are the three seismic force resisting systems available in AISI S400-20 [1]. All provide lateral resistance against the in-plane seismic forces and energy dissipation for the building during an earthquake.

Analysis of a recently assembled database of CFS framed shear walls and newly completed experimental studies show that significant overstrength, originating from both structural and non-structural detailing, exists when compared with the nominal strength as calculated per AISI S400-20 [2-6]. Recent wall-line tests show that the non-structural finish details can contribute considerably to the lateral resistance [7-9]. Shear wall testing also reveals that a ledger track can have an appreciable impact on the strength of a wall [10][11]. The influence of the ledger track and finish is not included in conventional CFS lateral design. Further, since only shear walls have designed tensile load paths for the chords (holdowns etc.), the lateral performance of full wall-lines may be sensitive to the location of the shear walls and tested specimens with unsymmetric locations of shear walls in a wall-line have featured modestly different response in opposite directions under dynamic loading [7-9].

Reliable nonlinear modeling is necessary to validate the seismic response modification coefficients, conduct advanced seismic design, and study the impact of modeling decisions on the lateral performance of CFS-framed buildings. The research herein employs a proposed advanced modeling framework to predict the lateral response of CFS-framed wall-lines, considering the effects of ledger tracks, finishes, and various other wall-line properties. The preliminary research results indicate that an adequately developed OpenSeesPy model can capture the impact of structural and non-structural detailing and different

[1] Graduate Research Assistant, Department of Civil and Systems Engineering, Johns Hopkins University, Baltimore, zhidongzhang@jhu.edu
[2] Research Structural Engineer, National Institute of Standards and Technology, matthew.speicher@nist.gov
[3] Graduate Research Assistant, Department of Structural Engineering, University of California, San Diego, ams082@eng.ucsd.edu
[4] Professor, Department of Structural Engineering, University of California, San Diego, tara@ucsd.edu
[5] Professor, Department of Civil and Systems Engineering, Johns Hopkins University, schafer@jhu.edu

wall configurations. The model proposed in this research can potentially be incorporated into future building-level numerical studies. The modeling protocol is being used to study the lateral performance of CFS-framed wall-lines observed in shake table tests [7-9] and provide recommendations on corresponding Performance Based Seismic Design (PBSD) procedures.

2. Recent Testing on CFS-framed Steel Sheet Wall-line

A series of CFS-framed wall-lines, with steel sheet sheathed shear walls within the wall-line, were recently tested through (a) a series of ground motions scaled to approximate different performance levels: elastic, quasi-elastic, design, and "above" design, and (b) through a quasi-static lateral loading [7-9]. The wall-line dynamic testing program was performed at the National Hazards Engineering Research Infrastructure (NHERI) outdoor shake table at the University of California - San Diego. Two pairs of wall-lines were tested on the shake table at the same time. Each pair had the same wall-line configuration and shared a top mass composed of a concrete slab and steel trench plates. The shake table applied excitation along the wall-line (long direction). After dynamic testing, selected specimens were subjected to slow monotonic loading to failure. Each wall-line specimen consists of four wall segments, each segment 1.2 m long. Utilizing the baseline specimen SGGS-1 nomenclature as an example (shown in Fig. 1, "S" is the abbreviation for "Shear wall segment", "G" stands for "Gravity wall segment", and "1" implies "Type-I shear wall".

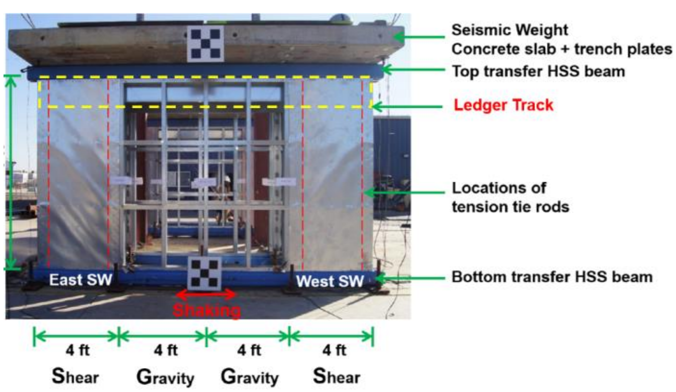

Figure 1: Baseline specimen on UCSD shake table (SGGS-1).

3. OpenSeesPy Model

A phenomenological finite element modeling framework is developed utilizing OpenSeesPy [12][13], a Python 3 interpreter of OpenSees. The finite element model for the baseline test specimen SGGS-1 features a ledger track and no finish system, and is used as an example to explain the model (provided in Fig. 1). The model employs displacement-based beam-column line elements for all framing members including studs and tracks, as shown in Fig. 2a. The section aggregator command is employed to define axial and flexural behaviors separately for the beam-column elements. For field studs and tracks, an elastic-perfectly plastic (EPP) material model (scaled to actual nominal strengths) is applied to capture the nonlinear axial and flexural behavior. The peak strength is determined per AISI S100-16 [14], thereby considering local buckling, distortional buckling, and yielding. The chord studs use a more sophisticated nonlinear model that employs a complete four-point backbone with a descending branch for both local buckling and distortional buckling as defined per Section 9.8 in ASCE 41-17 [15]. Note, global buckling behavior is captured by discretizing the studs into multiple beam-column elements over the unbraced length. Most elements use centerline definitions only; however, the ledger track web height (0.3 m) within the baseline specimen SGGS-1 is explicitly modeled with additional beam elements (0.3 m long) perpendicular to and rigidly connected to the horizontal beam element modeling the long ledger track itself. This allows the ledger-to-stud connection to transfer moment across the full depth of the ledger as opposed to a single point, thus providing a more realistic potential transfer of moment between these elements. Tie rods are modeled with truss elements and EPP material to capture tensile yielding and compression buckling.

The steel sheet sheathing in Fig. 1 is simulated with a pair of diagonal truss elements (Fig. 2a) utilizing a Pinching4 hysteretic model, which is calibrated via independent CFS-framed steel sheet sheathed shear wall cyclic test data [16]. Shear wall specimen CW2, from the [16], is selected as the closest configuration (similar framing thickness, sheathing thickness, and fastener spacing) compared with the SGGS-1 wall-line test. However, test CW2 is 2.44 m tall, while the SGGS-1 wall-line is 2.74 m tall. The static peak strength is scaled by 1.15 to accommodate energy-based cyclic degradation, which is included in the model. When non-structural finish is included, additional diagonal truss elements with the Pinching4 hysteretic model are incorporated for all the shear and gravity wall segments in the wall-line. The Pinching4 parameters for the gypsum finish are obtained from cyclic tests of CFS-framed walls with only gypsum boards [17]. Where required, the Pinching4 hysteretic model strength parameters for the Exterior Insulation Finishing System (EIFS) are scaled based on the EIFS strength back calculated from wall-line tests with and without finish [8] while other Pinching4 hysteretic parameters are set the same as the former gypsum finish.

A pushover analysis is conducted for the baseline SGGS-1 specimen. Fig. 2b provides the SGGS-1 specimen's base shear versus top track drift response when subjected to the design level earthquake followed by a slow monotonic pull test to just beyond 40 % strength drop from peak [7-9]. The base shear versus drift behavior generated by the numerical pushover simulation is also shown in Fig. 2b, exhibiting a post-peak difference of approximately 25 kN (15% of the peak strength value).

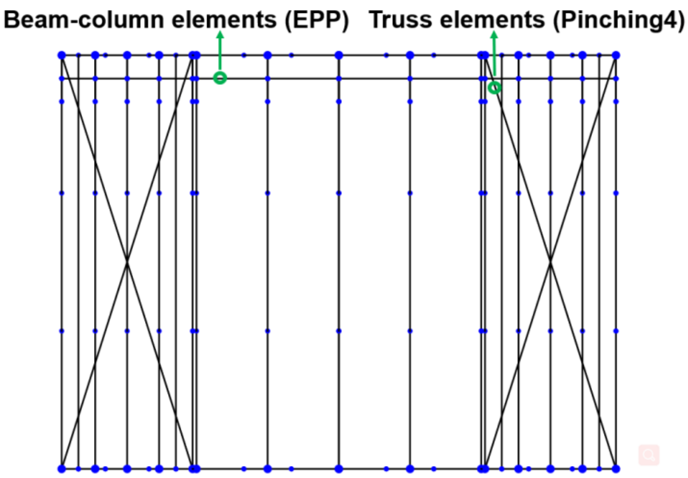

(a) OpenSeesPy finite element model

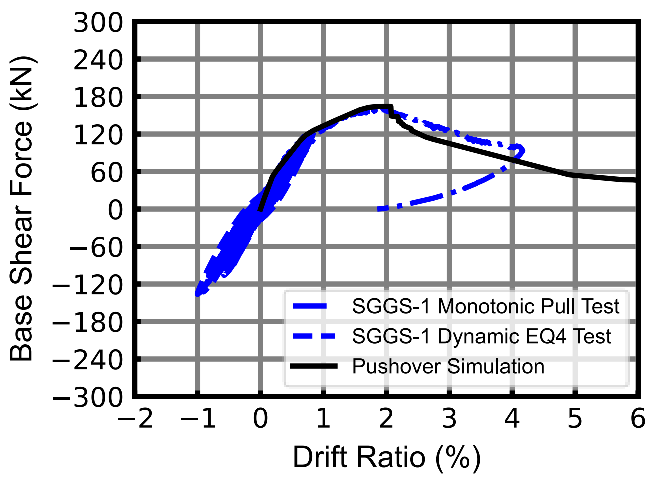

(b) OpenSeesPy model validation

Figure 2: OpenSeesPy finite element model and numerical model validation.

4. Impact of Ledger Track and Finish System on Wall-line Performance

In addition to the model for the baseline specimen, three additional models are established to investigate the impact of the ledger track and finish system on the wall-line shear strength, stiffness, and ductility. The three models include (i) a model without ledger track or finish (therefore, all steel framing and sheathed sheet steel shear wall is included) and (ii-iii) a pair of models with finish, but with or without a ledger track. Simulation results for all four models are provided in Fig. 3. The response of the walls without finish is provided in Fig. 3a and with finish in Fig. 3b. The corresponding moment diagram generated from the baseline specimen (SGGS-1) simulation is provided in Fig. 3c. The key strength and ductility parameters are tabulated in Table 1. Based on Fig. 3a and 3b, the peak strength of the monotonic pull tests and the elastic stiffness of the low intensity dynamic tests are utilized as a reference. Pushover simulation results for the two cases with a ledger track in Fig. 3a and 3b demonstrate reasonable agreement in the ultimate strength and initial stiffness compared with the tested wall-lines with a ledger track installed.

The model indicates that due to the presence of the ledger track, the wall-line strength changes by 47% in the unfinished case and 27% in the finished case, see Table 1. As shown in Fig. 3c, moment is present within the studs and ledger track due to the existence of the ledger track even though all the stud-to-top and bottom track connections and bracing-to-framing connections are modeled as pins. This additional moment increases the wall-line shear resistance. Further, in the model, the presence of finish systems on the wall-line further increases the modeled wall-line strength by 67% compared to a model without a ledger and 45% to a model with a ledger. In the model, the presence of a ledger track increases the initial stiffness, surprisingly due to the drift required to develop the bending capacity of the stud-to-ledger track connection, it also increases the ductility, with the drift at peak lateral force increased by 22% for the unfinished case and 13% for the finished case.

The nominal shear strength of the wall-line test baseline specimen is not available in Table E2.3-1 in AISI S400-20, thus the overstrength ratio in Table 1 is defined as the ratio of the simulation peak strength over the expected isolated shear wall test strength. The isolated test strength is based on specimen "CW2" in [16], modified to account for the presence of two 1.2m long shear walls in the wall-line, resulting in an expected shear strength of 100 kN. The static pushover overstrength ratio of the SGGS-1 baseline model is 1.12. The addition of the ledger track increases the overstrength ratio by 37% and addition of the finish increases overstrength by 56%, on average.

A piecewise linear backbone curve with elastic, hardening, and negative-stiffness segments plus a final residual plateau that terminated with a drop to zero strength has been proposed in the literature to calibrate the force-displacement backbone [18]. The wall-line base shear force-drift relationship can be fit to a piecewise linear backbone curve and the residual plateau (residual force ratio) can be a measure of ductility. The residual force ratio at 5% drift is adopted herein to evaluate the post-peak performance, with larger values implying that the structure is more ductile. The computed residual force ratios indicate that the presence of a ledger track increases the residual force ratio by 92%, while the finish increases it by 57%, on average.

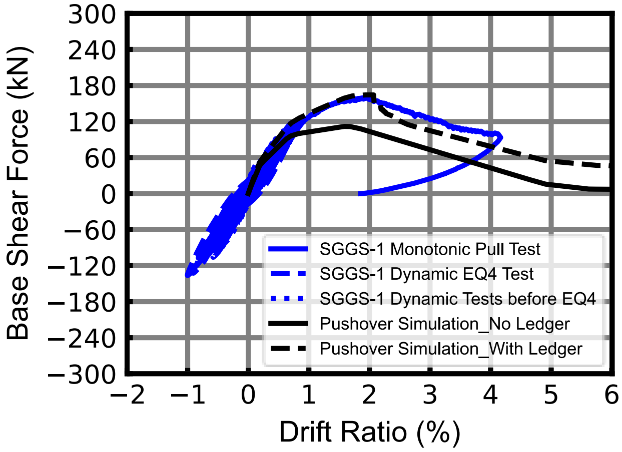

(a) Unfinished shear wall-lines

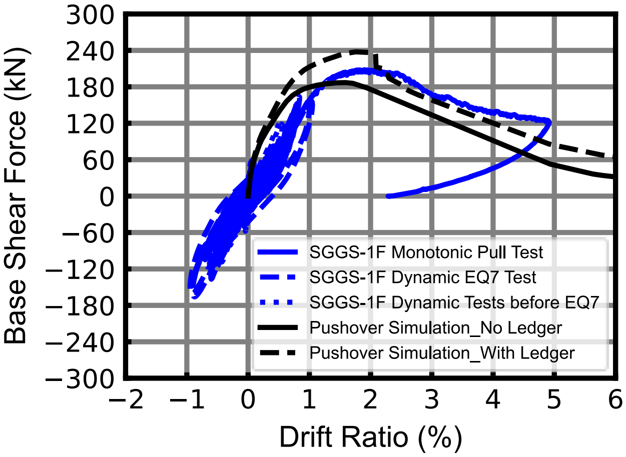

(b) Finished shear wall-lines

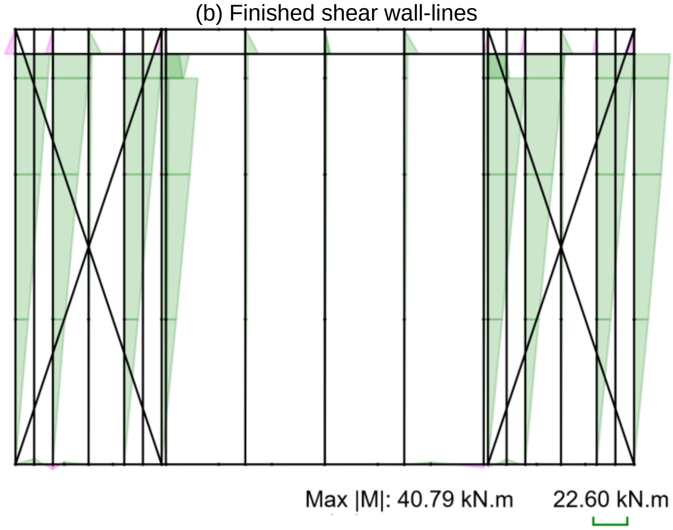

(c) Moment diagram @ peak load

Figure 3: Base shear force-drift relationship and a moment diagram of OpenSeesPy simulations.

Table 1: OpenSeesPy simulation result statistics summary.

Wall-line Configuration	Strength (kN)	Drift [a] (%)	Over-strength Ratio[b]	Residual Force Ratio[c]
Unfinished, no ledger	112	1.6	1.1	0.13
Unfinished, with ledger	164	2.0	1.7	0.33
Finished, no ledger	187	1.6	1.9	0.27
Finished, with ledger	238	1.8	2.4	0.35

[a] Drift ratio @ peak load
[b] Ratio of simulation strength over shear wall CW2 test strength [16]
[c] Residual force ratio @ 5% drift
[d] Only two validation results ("SGGS-1" and "SGGS-1F" wall-lines) are presented in this paper. Full suite of model validation against corresponding wall-line tests are presented in [19], including the simulation prediction-to-test strength ratio and corresponding uncertainty statistics.

5. Impact of Additional Wall-line Properties

A representative 17 m wall-line based on typical statistics for CFS buildings and scaled to force levels consistent with the 6th floor of an individual ten-story CFS framed building archetype [20] is selected to study the impact of additional wall-line properties on lateral performance. The wall-line consists of two 2.44 m shear wall segments, eight 1.22 m long gravity wall segments, and one 2.44 m window opening segment. Fig. 4 presents one symmetric and one unsymmetric configuration for this potential wall-line. As before, shear wall segments are denoted as "S". Tie-down (steel tie-rods in this case) component locations are indicated as short thick red lines as in Fig. 4. Gravity wall segments ("G") or window opening segments ("W") in Fig. 4 are not specifically designated to resist lateral loading, and thus they do not have explicit tie-down components.

As long as the length of shear wall remains the same current CFS design would assume any permutation of S, G, and W wall-line segments would provide the same strength. Two extreme wall-line cases are proposed in Fig. 4. The first is a symmetric wall-line with the shear wall "S" segment arranged at each wall-line ending boundary, as presented in Fig. 4a. The second is an unsymmetric wall-line with both shear wall "S" segments arranged at one wall-line ending boundary, as shown in Fig. 4b. The unsymmetric wall-line configuration does not have an explicit tie-down force path on the ending boundary without shear wall segments. Hypothetically the symmetric wall-line with boundary shear walls can utilize the lateral strength of the interior gravity walls effectively, while the asymmetric case having the shear walls on one side is more likely to only be able to develop the shear wall strength alone. It is worth noting that even without an explicit tie-down, the bottom track is connected to the floor below with regularly spaced anchors; however, it has been commonly assumed that such anchors will be ineffective in tension since they are (a) not explicitly designed for tension and (b) if engaged involve weak-axis bending of the track – which is limited.

In some cases the unsymmetric wall-line can develop similar capacities to the symmetric wall-line; therefore a sensitivity study was carried out to explore this condition.

The study considered: (a) low, medium, and high levels of track flexural rigidity (combined with floor diaphragm flexural rigidity), (b) spacing of the track shear anchorage (i.e., Powder-Actuated Fastener (PAF) spacing), and (c) magnitude of the gravity load level as summarized in Table 2.

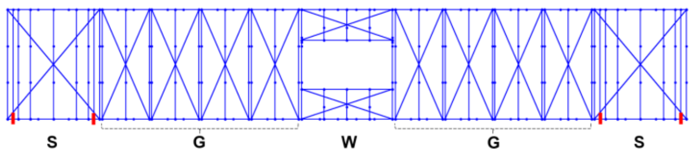

(a) Symmetric wall-line configuration

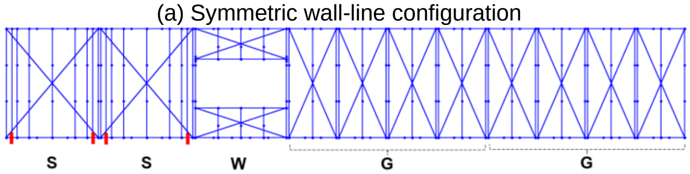

(b) Unsymmetric wall-line configuration

Figure 4: Representative wall-line configurations.

Table 2: Wall-line configuration parameter effects sensitive study matrix.

Effect	Low	Medium	High
Shear Anchorage (PAF) Spacing	One PAF every four studs	One PAF every two studs	One PAF between two studs
Gravity Load	1% × (1.05D+0.25L) [a]	25% × (1.05D+0.25L)	1.05D+0.25L
Track Bending Rigidity (EI)	EI_{Track} [b]	50 × EI_{Track}	1000 × EI_{Track}

[a] D implies dead load, and L means live load

[b] I_{Track} is the moment of inertia of cold-formed steel track

Following Table 2, 27 pushover analyses for the unsymmetric wall-line numerical models with various property combinations were conducted. The pushover direction is to the left in the figures ("tension" for the gravity end segments). The deformation patterns with a scale factor of 10 after pushover analysis are provided in Fig. 5a and Fig. 5b. The weakest strength case is shown in Fig. 5a, where the lateral strength of the gravity wall segment cannot engage the full wall-line lateral peak strength, because of a lack of a tie-down force path at the right wall-line boundary. However, in most cases the wall-line is able to develop full or close to full strength. A representative deformation pattern for the cases where the tie-down force loading path is fulfilled by one of the three conditions is provided in Fig. 5b. In Fig. 5b, all the wall segments are contributing to the overall wall-line lateral strength. The base shear force-drift relationship of the sensitivity study simulation results are provided in Fig. 5c. The study shows that if any one of the following three conditions is met: (1) shear anchor spacing is not larger than 0.6m (2 ft); or (2) track flexural rigidity (combined with floor diaphragm flexural rigidity) is not less than 50EI_{track}; or (3) the gravity load is not less than the design level 1.05D+0.25L, then the unsymmetric wall-line shear strength is close to the summation of the lateral strength of all wall segments considering gravity wall segments' and finish systems' contribution, regardless of the unsymmetric wall-line configuration. Therefore, the strength difference caused by the lack of tie-down force path can be ignored under certain, and potentially relatively common, wall-line properties.

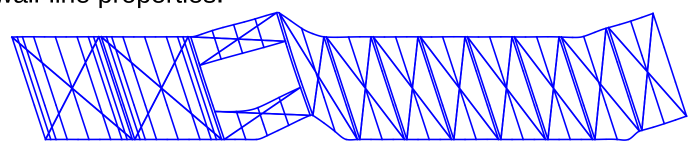
(a) Low gravity, low track stiffness, large PAF spacing case

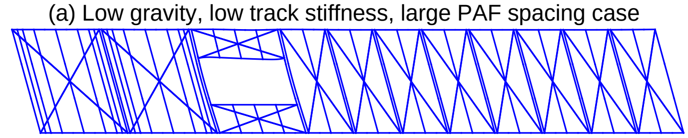
(b) High gravity, High track stiffness, medium PAF spacing case

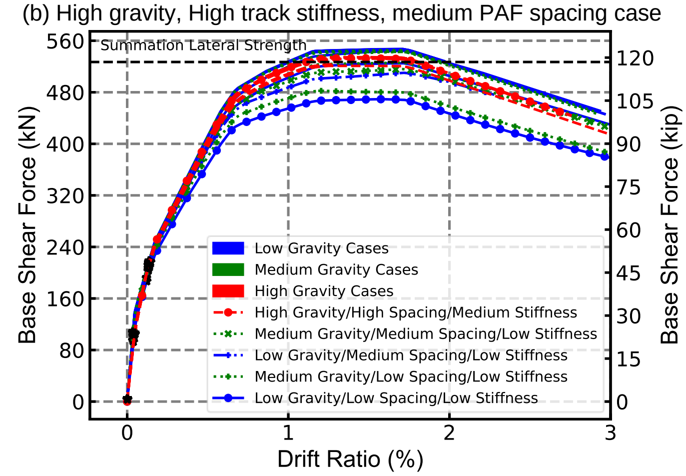

(c) Base shear-drift relationships based on simulation results

Figure 5: Representative deformation patterns and all the base shear force-drift relationship of sensitivity study simulation results.

6. Conclusions

This research utilizes OpenSeesPy to develop a modeling framework to capture the impact of structural and non-structural detailing for cold-formed steel (CFS) framed wall-lines that include steel sheet sheathed shear walls. Four OpenSeesPy models with and without ledger tracks and with and without finish systems are detailed. Simulation results indicate that both strength and ductility of the shear wall-lines increase due to the presence of ledger tracks and finish systems. The strength and ductility increase can be attributed to shear resistance provided by the finish system and moment restraint provided by the ledger-to-stud connection. A sensitivity analysis was conducted to explore the effects of additional wall-line properties including location of shear walls in a wall line, track bending stiffness, bottom track shear anchor spacing, and gravity loading. The analyses show that wall-line strength is insensitive to shear wall strength if any of the following is true: (1) shear anchor spacing is not larger than 0.6m (2 ft); or (2) track flexural rigidity (combined with floor diaphragm flexural rigidity) is not less than $50EI_{track}$; or (3) gravity load is not less than the design level 1.05D+0.25L. The modeling framework herein can be incorporated into future building-level simulations and used to help understand the impact of overstrength on the seismic performance of CFS shear wall systems.

7. Acknowledgments

The research is funded by the National Institute of Standards and Technology (NIST) Professional Research Experience Program (PREP) and the National Science Foundation (NSF) under Grant No.1663348 and No.1663569. Experiment data is contributed by the project Seismic Resiliency of Repetitively Framed Mid-Rise Cold-Formed Steel Building (CFS-NHERI). The authors thank Hernan Castaneda and Dr. Kara D. Peterman for their help in this work. Any opinions, findings, and conclusions or recommendations expressed in this material are those of the author(s) and do not necessarily reflect the views of NIST and NSF.

References

[1] AISI S400-20, North American Specification for Seismic Design of Cold-Formed Steel Structural Systems. Washington, DC, U.S.A.: AISI, 2015.

[2] D. Ayhan, S. Baer, Z. Zhang, C. A. Rogers and B. W. Schafer, "Cold-Formed Steel Framed Shear Wall Database," Proceedings of the Int'l. Spec. Conf. on Cold-Formed Steel Structures. St. Louis, MO, 2018.

[3] F. Haghpanah and B. W. Schafer, "Updated Fragility Functions for Cold-Formed Steel Light-Frame Structural Systems," Proceedings of the 12th National Conference on Earthquake Engineering. Quebec City, June 17-20, 2019. 8 pp, 2019.

[4] B. W. Schafer, Z. Zhang and F. Haghpanah, "Overstrength in seismic design of cold-formed steel framed shear walls," Cold-Formed Steel Research Consortium (CFSRC) Colloquium, 2020.

[5] Z. Zhang, C.A. Rogers and B. W. Schafer, "Cold-Formed Steel Framed Shear Wall Resistance Factors," Proceedings of the 12th National Conference on Earthquake Engineering. Quebec City, June 17-20, 2019. 8 pp, 2019.

[6] S. Mohebbi, S.R. Mirghaderi, F. Farahbod, A.B. Sabbagh and S. Torabian, "Experiments on seismic behavior of steel sheathed cold-formed steel shear wall cladded by gypsum and fiber cement boards," Thin-walled Structures, vol. 104, pp. 238-247, 2016.

[7] A. Singh, X. Wang, Z. Zhang, F. Derveni, H. Castaneda, K. D. Peterman, B.W. Schafer and T. C. Hutchinson, "Steel sheet sheathed cold-formed steel framed in-line wall systems. I: Impact of structural detailing," Journal of Structural Engineering, vol. 148, no. 12, 04022193, 2022.

[8] A. Singh, X. Wang, Z. Zhang, F. Derveni, H. Castaneda, K. D. Peterman, B. W. Schafer and T. C. Hutchinson, "Steel sheet sheathed cold-formed steel framed in-line wall systems. II: Impact of nonstructural detailing," Journal of Structural Engineering, vol. 148, no. 12, 04022194, 2022.

[9] A. Singh, T. C. Hutchinson, X. Wang, Z. Zhang, B. W. Schafer, H. Castaneda, F. Derveni and K. D. Peterman, "Wall Line tests: phase 1 -- shake table tests. CFS-NHERI: Seismic Resiliency of Repetitively Framed Mid-Rise Cold-Formed Steel Buildings," DesignSafe-CI, 2021. DOI: 10.17603/ds2-mvj8-8386.

[10] P. Liu, K. D. Peterman, C. Yu and B. W. Schafer, "Cold-formed steel shear walls in ledger-framed buildings," In Annual Stability Conference, Structural Stability Research Council, vol. 4, no. 1, pp. 27-47, 2012.

[11] P. Liu, K. D. Peterman, C. Yu and B. W. Schafer, "Characterization of Cold-formed Steel Shear Wall Behavior under Cyclic Loading for the CFS-NEES Building," International Specialty Conference on Cold-Formed Steel Structures, 2012.

[12] S. Mazzoni, F. McKenna, M. H. Scott and G. L. Fenves, "OpenSees command language manual," Pacific Earthquake Engineering Research (PEER) Center, 264, 2006.

[13] M. Zhu, F. McKenna and M. H. Scott, "OpenSeesPy: Python library for the OpenSees finite element framework," SoftwareX, 7, pp.6-11, 2018.

[14] AISI S100-16, North American Specification for the Design of Cold-Formed Steel Structural Members. Washington, DC, U.S.A.: AISI, 2016.

[15] ASCE/SEI 41-17, Seismic Evaluation and Retrofit of Existing Buildings. Reston, VA, U.S.A.: ASCE, 2017.

[16] R. Rizk and C.A. Rogers, "Higher strength cold-formed steel framed steel shear walls for mid-rise construction," Res. Rep., Dept. of Civil Engineering and Applied Mechanics, McGill Univ., Montreal, 2017.

[17] D. Morello, "Seismic performance of multi-storey structures with cold-formed steel wood sheathed shear walls," Master Thesis, Dept. of Civil Engineering and Applied Mechanics, McGill Univ., Montreal, 2009.

[18] D. Vamvatsikos and C. A. Cornell, "Direct estimation of the seismic demand and capacity of MDOF systems through incremental dynamic analysis of an SDOF approximation," ASCE Journal of Structural Engineering, vol. 131, no. 4, pp. 589-599, 2005.

[19] Z. Zhang. (2023). Simulation and Performance of Steel Sheet Sheathed Shear Walls in CFS-Framed Building Systems [Doctoral dissertation]. John Hopkins University.

[20] ClarkDietrich Engineering Design Inc. CFS-NHERI 10 Story Archetype Design, 2021.